

# UTILIZATION OF CARBON NANOTUBE AND DIAMOND FOR ELECTRON FIELD EMISSION DEVICES

Phan Ngoc Minh<sup>1,\*</sup>, Phan Ngoc Hong<sup>1</sup>, To Manh Cuong<sup>1</sup>, Takahito Ono<sup>1</sup> and Masayoshi Esashi<sup>2</sup>

<sup>1</sup> Graduate School of Engineering, <sup>2</sup> New Industry Creation Hatchery Center, Tohoku University  
01AzaAoba, Aramaki, Aoba-ku, Sendai 980-8579, Japan

Tel. 81-22-217-6256; Fax. 81-22-217-6259; Email: [minh@mems.mech.tohoku.ac.jp](mailto:minh@mems.mech.tohoku.ac.jp)

(\* Also with Institute of Materials Science, Vietnam National Center for Natural Science and Technology)

## ABSTRACT

We are currently developing a monolithic electron field emission device and integrated electron optic components for multi-electron beam lithography microsystems basing on a SOI (Silicon On Insulator) wafer. In the Transducer'03 conference, we have reported the concept, simulation, fabrication, emission and focusing characteristics of the device with Pt, Mo emitters [1].

In this paper, we propose an advanced structure with the integration of the focusing, beam correction (stigmator) electrodes and metallic ring array for detection of secondary electrons emitted from the wafer. Initial results of utilizing boron doped diamond and carbon nanotubes (CNTs) emitters are presented. Both diamond and the CNTs were selectively grown using a hot-filament chemical vapor deposition (HF-CVD) technique. Results of field emission improvement of the bundle CNTs on a Si tip array by hydrogen (H<sub>2</sub>) treatment are demonstrated. The improvements of the emission current and the long-term stability were attributed to the reduction of the CNTs work function by the formation of C-H bonds.

## 1. INTRODUCTION & MOTIVATION

Currently, DUV (Deep Ultraviolet) photolithography of 90 nm node is used for Large Scale Integrated circuits (LSI) technology, that enables to make IC of 330 millions transistors/chip or 120 billions transistors/300 mm wafer [2]. To reduce feature size, increase the density and performance of electronic devices, photolithography using Extreme Ultra Violet light, and others alternative lithography techniques using such as X-ray, scanning probes, and optical near-field were proposed for next LSI. These techniques, however have some serious limitations, require high complexity of the system, specialized optics and high cost.

Electron beam lithography (EBL) offers high resolution of the range 10-100 nm but very low production rate for the LSI. A number of groups have been trying to develop high throughput EBL systems. Chang, et al. has proposed a concept of multi EBL by assembling an array of STM tips with a miniaturized electron lens array [3]. A 20x20 mm footprint microcolumn with a single tip for 100 nm lithography was demonstrated [4]. Recently, there are a number of projects to approach the parallel EBL, for instance,

European IST project "Nanolith" for developing a system of 32 microguns [5]. To our best knowledge, the utilization of the multi-beam system was not achieved yet due to many technological difficulties.

We are developing a novel micromachined device basing on the SOI wafer and carbon based materials for the multi-electron beam lithography system as shown in Fig. 1. The advantages of our device are the following. All components (emitters, gate, focusing, stigmator electrodes, and isolation layers) can be monolithically fabricated in a batch process without any assembling steps and such components can be self-aligned together. A control IC chip can be bonded to the device using a glass substrate with high density electrical feed-throughs. Various materials for emitter, especially, doped diamond or individual Carbon Nanotubes (CNT) emitters of ultra small size, high brightness, low energy spread, low threshold voltage can be selectively formed. An array of metallic rings at the lower side of the device can enable to detect secondary electrons emitted from the wafer as a multi-SEM system. A simulation work presented in previous report has shown that at the gate voltage=100V, anode voltage=1kV, lens voltage=-6V, the emitted electron beam can be focused in a

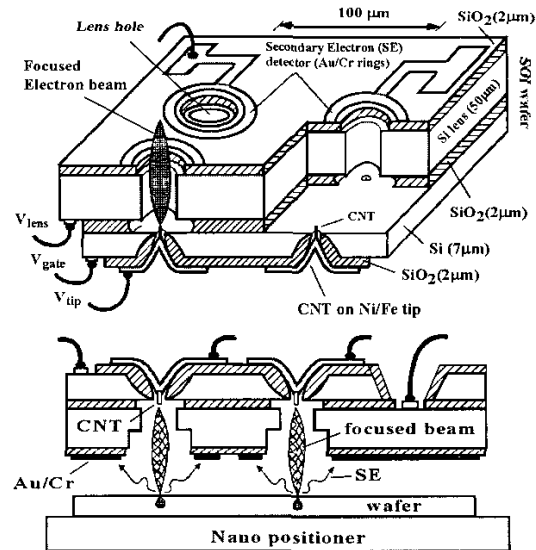


Figure 1: Schematic structure of the device.

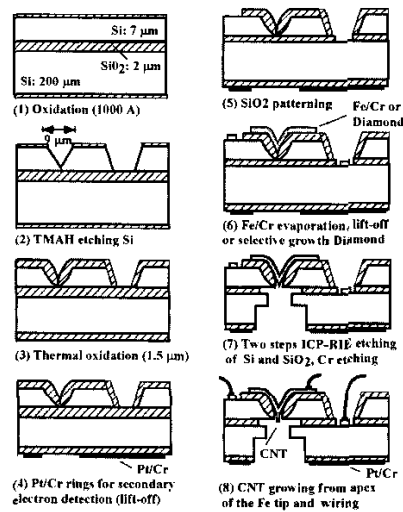


Figure 2: Fabrication procedure.

40 nm spot and focal length=250  $\mu\text{m}$  [1]. The simulated results and advantages of the fabrication process strongly motivated us in realization of the device.

To reduce the spherical and chromatic aberrations and focus the beam into a small spot, electrons should be emitted from an ultra-small source with low energy spread and electron microoptic components must be perfectly symmetry. Recently, carbon nanotubes (CNTs) were known as an ideal material for field emitter. Many basic researches showed that the CNT with its small radius (1-20 nm) and high aspect ratio structure could emit electrons with high brightness, low energy spread (0.18 eV), low threshold voltage (1 V/ $\mu\text{m}$ ) and stable emission stability [6-8]. Diamond material was also a good candidate for field emitter due to the negative electron affinity that can lower the threshold voltage. Diamond is chemical inertness and high hardness material so it can withstand the ion bombardment effect and improve emission stability. These excellent emission properties and the possibility of fabrication process strongly motivated us in utilizing individual CNT and diamond as the emitter for our devices.

## 2. FABRICATION, CHARACTERIZATION

Shown in Fig. 1 is schematic view and principle of the device. The device consists of independently addressable emitters, a common Si gate electrode, electrostatic Si lenses, stigmators and an array of Au/Cr or Pt/Cr rings for secondary electron detection. The distance between emitters were designed at 100-200  $\mu\text{m}$ . Lens hole diameters and height were 50-100  $\mu\text{m}$  and 50-70  $\mu\text{m}$ , respectively. Isolation layers were thermal  $\text{SiO}_2$  of 2  $\mu\text{m}$ -thick. Gate holes were 1-2  $\mu\text{m}$ -diameter. To perfectly correct the focused beam, 4 stigmator electrodes were also formed at the substrate side of the wafer by dry etching. The focus and stigmator electrodes were isolated by 30  $\mu\text{m}$  air gap (not shown here).

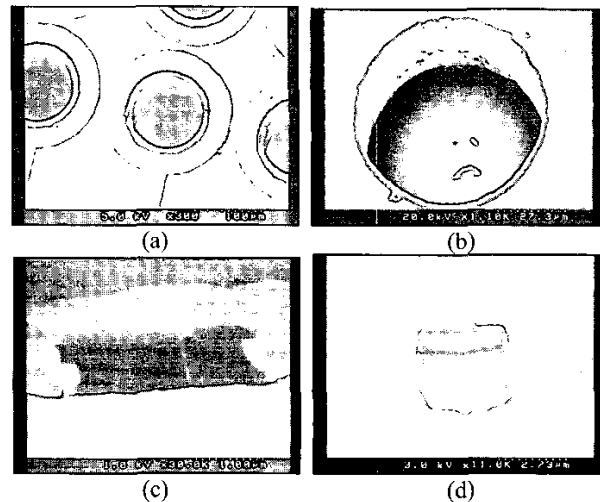


Figure 3: SEM images of the fabricated device (a) Si lens with Pt/Cr ring for electron detection; (b) Close up view of Si lens; (c) Close up view of the gated individual CNT and (d) Close up view of the doped diamond emitter.

The fabrication process of the device is shown in Fig. 2. Basically, it is identical to the process presented in Ref. 1. The differences are the formation of metallic ring array for electron detection (step 4), selective growth of the diamond emitter (step 6) and the utilization of Fe catalyst tip for the growth of the CNTs (steps 6-8). Briefly, steps 1-2: forming etch pits on the Si active layer of the SOI by photolithography and wet etching in a TMAH; step 3: thermal oxidation of 1.5  $\mu\text{m}$ -thick  $\text{SiO}_2$ ; step 4: forming array of Pt/Cr rings on the  $\text{SiO}_2$  layer of the Si substrate by lift-off process; steps 5-6: forming Fe/Cr (300 nm/30 nm) tips by lift-off or selective growth of diamond; step 7: forming array of cylindrical columns and stigmators at the substrate by reactive ion etching,  $\text{SiO}_2$  etching to expose the emitters and etching Cr at the apex of the emitter. Since the height of the lens was optimized at 50-70  $\mu\text{m}$ , dry etching in two steps was done at step 7. Finally, CNT was selectively grown at the apex of the Fe tips in the HF-CVD at 600°C-750°C in 30 Pa pressure of  $\text{H}_2:\text{C}_2\text{H}_2$  (1:99) mixture. During the growing process, a negative voltage of 300 V was applied between the Fe tips and a filament located at 5 mm above the sample [8]. The boron doped diamond emitter array was selectively grown in the HF-CVD at 950°C in 5.2 KPa pressure of  $\text{H}_2:\text{CH}_4$  (1.5:98.5) and vaporized trimethoxyborane doping source mixture [9].

Fig. 3 shows several illustrations of the fabricated device: (a) SEM image of the Si lens with Pt/Cr electron detection ring array; (b) close up view of the Si lens of 60- $\mu\text{m}$ -diameter and 50  $\mu\text{m}$ -height and visible gated emitter; (c) SEM image of the individual CNT grown at the gated Fe tip; (d) close up view of the gated diamond emitter. A Raman study has shown that the grown diamond tip was mainly  $\text{sp}^3$  configuration. Depending on the shape of the Fe tips and conditions of the growth, bundle CNTs were also grown under the Si gate as shown in Fig. 4a.

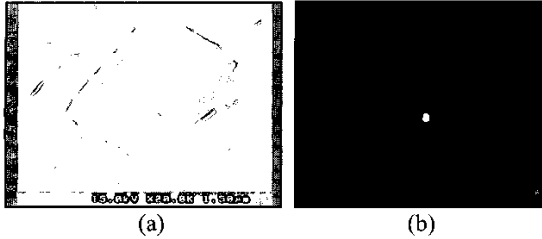


Figure 4: (a) SEM image of the gated bundle CNT and (b) corresponding emission pattern observed by the phosphor screen (spot size: 200  $\mu\text{m}$ ).

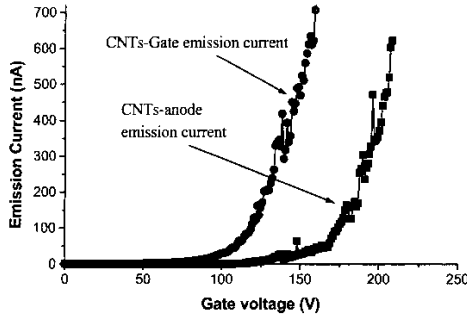


Figure 5: Emission and gate leak current as a function of the gate voltage of the device with bundle CNTs emitter.

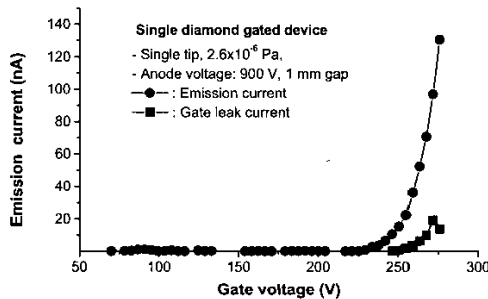


Figure 6: Emission and emitter-gate leak current as a function of the gate voltage of the device with single boron doped diamond emitter.

Electron emission current and emission pattern were measured in an UHV chamber. Fig. 4b shows electron emission pattern observed at a phosphor anode screen for the bundle CNTs (Fig. 4a) at a tip-screen distance of 1 mm, and the gate voltage and anode voltage of 200 V and 1 kV, respectively. The emission and emitter-gate leak current of the bundle CNT is shown in Fig. 5. It is seen that the grown bundle CNTs were randomly oriented under the Si gate hole. Therefore, electrons are mainly emitted toward the gate. A part of the emitted electrons reach the cathode with an emission pattern as shown in Fig. 4b. The emission pattern of the individual CNT was not successfully observed by the screen. These results, however, confirmed the feasibility of the selective growing technique of the CNT at the gated Fe emitters in the system. The individual CNT will be applicable

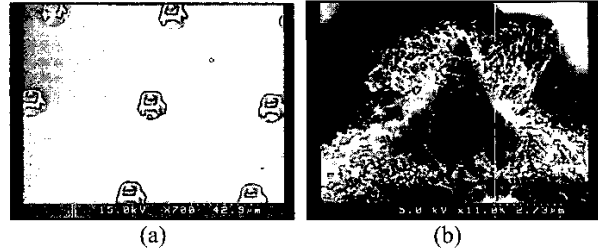


Figure 7: SEM image of the CNTs/Si tip array.

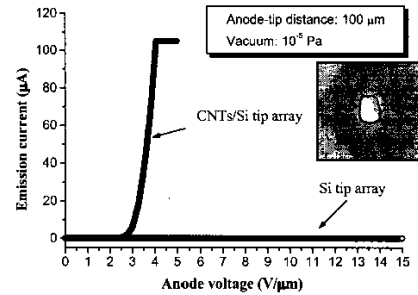


Figure 8: Emission current of the bundle CNTs/Si tip array ( $10 \times 10$ ) tips at the anode-tips distance of 100  $\mu\text{m}$ . (The inset shows the emission pattern at 400 V, 1.5x1.5 mm size).

in the device.

The emission current of the diamond emitter was measured using the same setup. Fig. 6 shows the emission and leak currents of the single diamond emitter in the array. It is seen from Fig. 6 that the threshold voltage and leak current was quite high ( $V_{th} \sim 220\text{V}$ ). The emission current was stable for several hours and then suddenly down because the increasing of the leak current through the gate at a high gate voltage (270 V). The high threshold voltage and low emission current of the grown diamond may be due to the lack of electrons in P-doped diamond. By doping diamond with N-type dopant, the emission characteristics could be improved. Importantly, the shape of the diamond tip was not changed after the measurement and breakdown.

### 3. IMPROVEMENT OF ELECTRON EMISSION OF THE CNTs EMITTERS

For practical application in lithography, besides reducing the spot size of the electron beam, it is very important to improve the stability ( $<1\%/h$ ) and life-time of the emission. According to J. Robertson [10], in carbon based materials, the stable C-H bonds can lower the electron affinity and greatly improve their emission performance. To study the possibility of improvement of the emission current,  $10 \times 10$  micromachined Si tips array was used as substrate for CNTs growth and their emission current was measured during Hydrogen treatment. Fig. 7 shows SEM images of the bundle CNTs/Si tip array and close-up view of one tip. The preparation of such sample was reported in Refs. 11-12. The grown CNT was multi-wall with diameter of about 20 nm.

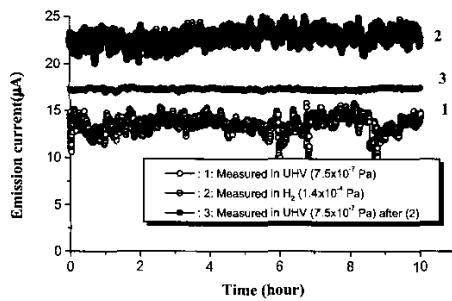


Figure 9: Improvement of emission stability of the bundle CNTs/Si by emission-induced H<sub>2</sub> treatment. Before (1), during (2) and after hydrogen treatment (3).

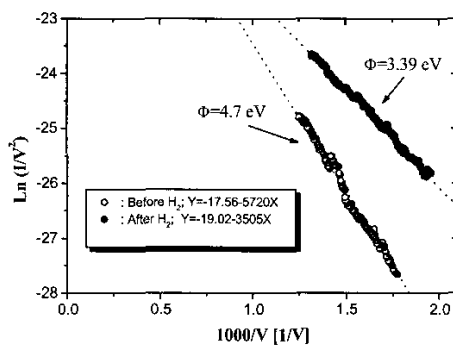


Figure 10: Fowler-Nordheim plot in the high emission current regime of the CNTs before and after introducing H<sub>2</sub>.

The emission current was measured in  $4 \times 10^{-7}$  Pa chamber by applying voltage between the sample and the phosphor anode screen located at 100  $\mu\text{m}$  distance. Fig. 8 shows the emission currents of the Si tip with and without CNTs. The inset in Fig. 8 shows emission pattern of the bundle CNTs/Si tips at 400 V. A large emission current over 0.1 mA with threshold voltage of 2.4 V/ $\mu\text{m}$  was found for the bundle CNTs/Si tips. The emission at a constant voltage was measured over a week in order to clean contamination, if any, by Joule heating until the emission current getting stable before introducing gases. The distance to the anode was then increased to 600  $\mu\text{m}$ , anode voltage=0.8 kV and kept constant during the emission process and introduce gas into the chamber through a leak valve. Fig. 9 shows time-variation of the emission current of the bundle CNTs/Si tip array measured in UHV (curve 1), in  $10^{-4}$  Pa H<sub>2</sub> (curve 2) and in  $10^{-6}$  Pa Vacuum after H<sub>2</sub> treatment (curve 3). It is clearly seen that the intrinsic environmental stability of the CNT was strongly improved (from 35% to below 3%). After H<sub>2</sub> treatment, the threshold voltage was reduced to 0.5 V/ $\mu\text{m}$ . By introducing O<sub>2</sub> or Air, the emission current was drastically reduced. The effect was reproducible with different testing samples. The measured emission current was well followed the Fowler-Nordheim (F-N) mechanism.

The F-N equation can be simply expressed as

$$\ln(I/V^2) = a - b/V \quad (1)$$

The slope (b) of the curve is expressed as:

$$b = 2.82 \times 10^7 (\Phi^{3/2}/\beta) \quad (2)$$

where,  $\beta$  ( $\text{cm}^{-1}$ ) is geometrical factor that strongly depends on the radius and geometry structure of the emitter;  $\Phi$  is work function of the emitter. By plotting  $\ln(I/V^2)$  vs.  $(1/V)$  in the high emission current regime, we received linear curves as shown in Fig. 10. By linear fitting these data, we received  $b_1 = -5720$ ,  $a_1 = -17.56$  and  $b_2 = -3505$ ,  $a_2 = -19.02$  the sample before and after H<sub>2</sub> treatment, respectively. Noted that, in this experiment, we did not thermal treat the sample in order to keep the emitters morphology unchanged and the applied electric field was quite low (800 V/600  $\mu\text{m}$ ) to ensure no back sputtering to the emitter. We consider that the geometrical factor  $\beta$  of the CNTs/Si tip before and after introducing H<sub>2</sub> is unchanged. Actually, no evidence for ion sputter damage was observed after the measurement. Consequently, we have the following relations

$$b_1/b_2 = (\Phi_1^{3/2}/\beta_1)/(\Phi_2^{3/2}/\beta_2) \quad (3)$$

$$\Phi_1/\Phi_2 = (b_1/b_2)^{2/3} \quad (4)$$

In considering the work function of the CNT,  $\Phi_1 = 4.7$  eV [10], we found  $\Phi_2 = 3.39$  eV. This work function reduction ( $\Delta\Phi = 1.13$  eV) may be due to the emission assisted surface reaction and formation of C-H bonds. As seen in Fig. 9, after treatment, the emission current of the CNT were more stable over 10 hours measurement. Similar results were observed for individual Carbon nanocoils on a W tip.

In conclusion, the observed results for the diamond and CNTs emitters are meaningful for our device. Such low voltage, multi beam, maskless, low cost and compact system are expected to operate in parallel to improve throughput of lithography.

## REFERENCES

- [1] P. N. Minh, et al., Technical Digest of the TRASDUCERS'03, Boston, USA, 2003, p. 1295-1298.
- [2] From <http://www.intel.com>
- [3] T. H. P. Chang, et al., IEEE Trans. On Electron Devices, Vol. 38, No. 10 (1991) 2284-2288.
- [4] E. Kratschmer, et al., J. Vac. Sci. Technol. **B14**, 1996, 3792-3796.
- [5] K. B. K. Teo, Vu Thien binh, et al., J. Vac. Sci. Technol. **B21**, 693-697 (2003).
- [6] J. M. Bonard, et al., Appl. Phys. A69, 245-254 (1999).
- [7] Niels de Jonge, et al., Nature **420**, 393-395 (2002).
- [8] P.N.Minh, et al., Jpn. J. Appl. Phys., 41, L1409 (2002).
- [9] J. H. Bae, et al., Technical Digest of the TRASDUCERS'03, Boston, USA, 2003, p. 778-781.
- [10] J. Robertson, J. Vac. Sien. Technol. **B17**, 659 (1999)
- [11] C. H. Tsai, et al, Technical Digest of the TRASDUCERS'03, Boston, USA, 2003, p. 770-773.
- [12] P. N. Minh, et al., J. Vac. Sien. Technol. **B21**, 1705-1709 (2003).